Broadband Permittivity and Permeability Extraction of 3-D-Printed Magneto-Dielectric Substrates

Jakub Sorocki, *Member, IEEE*, Ilona Piekarz, *Member, IEEE*, and Maurizio Bozzi, *Fellow, IEEE*

Abstract—A broadband microwave magneto-dielectric spectroscopy technique is introduced and dedicated to the characterization of 3-D-printed magneto-dielectric substrates. Complex permittivity and permeability are extracted for the material-under-test fabricated in the same manner and with the same orientation of the electro-magnetic (EM) field as in the intended applications that include, for example, miniaturized and efficient antennas. The information is derived from the measured characteristic impedance and propagation constant of a test microstrip transmission line. To exclude the influence of the coaxial-to-microstrip transitions, printed launchers are proposed with puzzle-like interlock to test substrate which is used together with a printed thru-reflect-line (TRL) de-embedding set. The presented technique was experimentally validated on an example of specialized magnetic polylactic acid (PLA) filament printed substrate in the frequency range 0.1–6 GHz and a reference PLA substrate measured with two different techniques to yield comparable results.

Index Terms—3-D printing, broadband material characterization, magneto-dielectric substrates, microwave circuits, miniaturized antennas.

I. INTRODUCTION

THE magneto-dielectric materials combining both dielectric and magnetic properties have been extensively studied in recent years for the realization of high-performance antennas [1], [2]. Such antennas can offer broader operational bandwidth, smaller physical footprint as the size reduction is proportional to the product of substrate permittivity and permeability, or improved radiation efficiency that is related to the permittivity and permeability ratio. On the other hand, the rapid development of additive manufacturing techniques and dedicated materials has opened a new realm of possibilities for highly integrated 2.5-D/3-D partially/fully printed RF electronics. Nevertheless, material characterization to establish its electrical parameters toward intended application is a critical step of the development process. The methods described in the literature for magneto-dielectric materials are mostly narrow-band resonant techniques [3], [4], which may serve as a cross-verification rather than the main source of information in broadband applications. This is especially important when

Fig. 1. Photograph of the test assembly for the proposed technique. A puzzle-like launcher (black material) is used at each end as an intermediate element between the end-inserted coaxial connector and microstrip line on the substrate-under-test (gray material). Launchers are then de-embedded to provide the measured *S*-parameters referenced at the test material edges.

a newly developed material is analyzed as, in general, a dispersive medium behavior is expected. One of the broadband characterization methods is the Nicolson–Ross–Weir method, which is a transmission/reflection type [5]. The properties of a non-conductive material are determined directly from the measured impedance and propagation constant. Nevertheless, the main drawbacks of this technique are the requirement for thickness, size, and shape of the sample along with the need for waveguide or coaxial measurement setup [6]. Another broadband approach that uses a more application-specific setting is, for example, the microstrip line method that uses a test line fabricated on a substrate being the material of interest [7]. Again, the information is extracted from the measured characteristic impedance and propagation constant of the line section; however, due to quasi-TEM propagation, a model that bounds medium effective and substrate relative properties is required. The main drawbacks of the method are the need for a sample with two-sided metallization to fabricate conductive strips and the use of a specialized test fixture, like in [8], to launch the wave from a coaxial line into a microstrip. Such fixtures introduce a discontinuity/impedance step of which must be de-embedded from measurements and usually accept a narrow range of substrate thicknesses.

In this article, we introduce a low-cost and test fixture-free method dedicated to the broadband characterization of printable magneto-dielectric materials. The technique explores the test microstrip line approach and takes advantage of conductor fabrication of [1] along with the flexibility of 3-D printing to realize not only the substrate-under-test but also puzzle-like coaxial-to-microstrip end launchers (see Fig. 1). Since transitions to launch the quasi-TEM wave are unavoidable, the attachable launchers make it easy to fabricate a kit and apply the thru-reflect-line (TRL) technique [9] to de-embed the measurements and provide *S*-parameters for the line section on the substrate-under-test only. From that, the complex permittivity and permeability are determined as in [7]. The proposed technique was experimentally validated on an example of 3-D printed substrates realized by the fused deposition modeling (FDM) technique out of specialized magnetic PLA filament and a reference PLA. A focus was put on the frequency range up to the 5.8-GHz industrial, scientific and medical (ISM) band where the magneto-dielectric materials are finding their use.

II. PERMITTIVITY AND PERMEABILITY DETERMINATION

The proposed broadband magneto-dielectric spectroscopy technique is centered around the microstrip line (modML) method, where a test line is fabricated on the substrate-under-test with extra coaxial-to-microstrip launchers. The substrate's intrinsic properties extraction method is based on processing the complex *S*-parameters measured at the substrate edges as reference planes (see Section III-A for de-embedding). It requires a microstrip line properties calculation (direct problem) together with an optimization procedure (inverse problem). Assuming the measured data describes a section of a uniform transmission line, then one can compute its *S*-parameters as

$$S_{11} = S_{22} = \frac{\left(Z_c^2 - Z^2\right)\sinh(\gamma l)}{\left(Z_c^2 + Z^2\right)\sinh(\gamma l) + 2 Z_c Z \cosh(\gamma l)} \quad (1a)$$

$$S_{12} = S_{21} = \frac{2 Z_c Z}{\left(Z_c^2 + Z^2\right)\sinh(\gamma l) + 2 Z_c Z \cosh(\gamma l)} \quad (1b)$$

where l is the physical length of the line, Z_c is its characteristic impedance, Z is the *S*-parameters reference impedance, and γ is its propagation constant. On the other hand, assuming the quasi-TEM mode dominant propagation, one can write simple formulas relating Z_c and γ with the properties of the propagation medium exhibiting both dielectric and magnetic properties

$$Z_c = Z_0 \sqrt{\frac{\mu_{\text{reff}}}{\varepsilon_{\text{reff}}}}; \quad \gamma = j \frac{2\pi f}{c_0} \sqrt{\varepsilon_{\text{reff}} \mu_{\text{reff}}} \quad (2)$$

where f is the frequency, c_0 is the free-space velocity of light, Z_0 is the characteristic impedance in the air (analytical expression in [10, eq. (1)]), while $\varepsilon_{\text{reff}}$ and μ_{reff} are effective permittivity and permeability of the microstrip stack up, respectively. Finally, one can find analytical relations bounding the substrate relative and medium effective properties considering the microstrip geometry (linewidth w and substrate thickness h). A dispersive effective equation for the electric case $\varepsilon_{\text{reff}}(\varepsilon_r, f)$ is found, for example, in [11, eq. (10)] while for the magnetic case $\mu_{\text{reff}}(\mu_r, f)$ in [7, eq. (5)]. Note that a duality relationship provides conversion $\varepsilon_r \rightarrow (1/\mu_r)$ and $\varepsilon_{\text{reff}} \rightarrow (1/\mu_{\text{reff}})$ and thus the latter is derived from the former.

Therefore, the effective parameters can be determined directly from the measured *S*-parameters by solving (2) for $\varepsilon_{\text{reff}}$ and μ_{reff}. Phase unwrapping must be applied for Im(γ) to ensure proper data. From that, the relative properties of the substrate are found for each frequency point numerically through the inverse optimization procedure, which simultaneously carries out the ε_r and μ_r computation and the convergence between measured values of $\varepsilon_{\text{reff}}$ and μ_{reff} and those computed analytically.

III. TEST SETUP DESIGN AND EXPERIMENTAL RESULTS

A. Coaxial-to-Microstrip Launcher and TRL Kit

The test setup is comprised of a microstrip line fabricated on the 3-D printed substrate-under-test with launchers attached at each end, which are necessary to transition from coaxial to microstrip guide. The extraction of the substrate intrinsic properties is assuming a uniform transmission line section while transitions introduce impedance step/discontinuity. Therefore, to match the algorithm assumptions and provide properly reference *S*-parameters, transition de-embedding is necessary. The
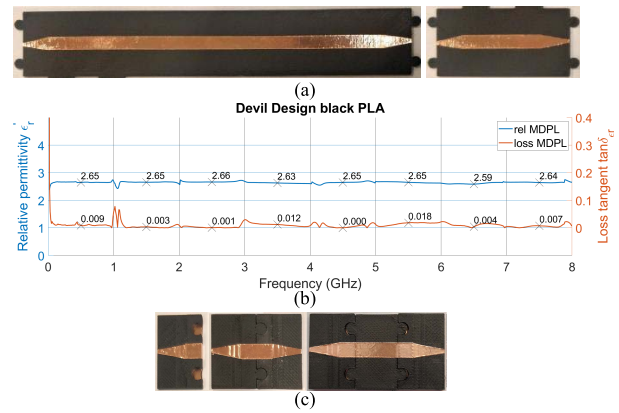

Fig. 2. (a) Photographs of the fabricated LL test lines (b) along with extracted complex relative permittivity of the material to be used for the line standard. (c) Photographs of the fabricated TRL kit: open, thru, and line.

proposed attachable printed launchers with a lego-like system for alignment make it easy to realize, for example, a TRL [9] de-embedding kit using the same fabrication technology as the substrate-under-test.

For the sake of experimental study, the launcher was designed and fabricated using the FDM technology along with the de-embedding TRL kit. An off-the-shelf, black PLA filament by Devil Design [12] was used for both launchers and the line standard. It is important to note that for the TRL algorithm, the de-embedded *S*-parameters reference impedance Z is set by the characteristic impedance of the line standard and thus special care must be taken in the choice of the material and the fabrication. Maintaining a known line impedance over its intended bandwidth is crucial for accurate determination of the test line Z_c.

Since the PLA is a dielectric material while filaments' electrical properties may vary depending on the additives, the selected one was characterized before designing the line standard using the microstrip differential phaselength (MDPL) method for which the line-line (LL) algorithm of [13] for γ determination and $\varepsilon_{\text{reff}}(\varepsilon_r, f)$ formula from [11] for permittivity extraction were used. The LL test substrates having lengths of 150 and 50 mm (for improved accuracy at low frequencies) and width of 25 mm were 3-D printed using the Prusa i3 MK3s 3-D printer by Prusa Research with 0.4-mm nozzle at 100% infill at 0.15-mm layer height and using Prusa Slicer default temperature profile for PLA. Total thickness was set at 1.55 mm to accept a 63-mil end-mounted subminiature version A (SMA) that can be press-fitted for solder-free connection. Metal strips for the microstrip line were realized using a fixed width, 25-μm-thick copper tape with adhesive backing: a 5-mm wide one (impedance in the vicinity of 50 Ω) for the top conductor and 25 mm wide for the ground plane. The conductor's ends were cut using a template to form a 1–5-mm wide, 10-mm long taper to accept the press-fitted printed circuit board (PCB) end-mounted SMA connectors and prevent shortening the center conductor. Due to the method's "difference" nature and used algorithm, neither taper nor line's impedance does not affect the extracted properties. The fabricated LL test lines along with the resulting nominal permittivity data (3σ uncertainty of ± 0.04) are provided in Fig. 2.

To realize a 50 Ω line standard using a 5-mm-wide tape, one needs a PLA substrate to be 1.85-mm thick assuming $\varepsilon_r = 2.65$. Moreover, a single, 14-mm-long line covers the 1–6 GHz

Fig. 3. Assembled test lines for FDM printed substrates: reference black PLA and magnetic iron PLA. The use of copper tape enables a seamless realization of the microstrip conductor.

band. Following, the launcher geometry was selected to be 25-mm wide, 15-mm long, and 1.55-mm thick at the connector side to accept a 63-mil end-mounted SMA and 1.85-mm thick at the other to match the line thickness. Finally, substrates for a set of launchers and the line were printed with the same settings as above in one run to maintain consistency, and the TRL kit was assembled [see Fig. 2(c)]. The same line's taper as before was added the influence of which is de-embedded.

B. Test Substrates and Permittivity/Permeability Extraction

For the sake of experimental verification of the method, two test substrates were fabricated: one out of the magnetic iron PLA filament by Protopasta [14] being an off-the-shelf magneto-dielectric material and one out of black PLA filament by Devil Design. The second substrate was used to cross-validate the resulting data against one obtained with a simpler LL test method. Both substrates were 2-mm thick by 25-mm wide by 150-mm long slabs. The same fabrication procedure and settings were used as previously. A 5-mm-wide tape was used to realize the top conductor in both cases. A photograph of the assembled test lines with snapped-on launchers is provided in Fig. 3.

All S-parameters for the test lines were measured at room temperature with the Agilent N5224A PNA vector network analyzer (10 MHz step, 1 kHz IF filter) and de-embedded using the fabricated kit. The fabricated lines were gauged to assess the uniformity and thickness of the substrate, width, and length of the line with a result that is very close to the design geometry and thus such was used. Then, the procedure described in Section II was applied to extract the complex permittivity and permeability. The resulting nominal data is provided in Fig. 4 with no post-processing. The periodic inaccurate peaks are due to procedure divergence at frequencies corresponding to integer multiples of one-half wavelength in the sample (small value of $|S_{11}|$) and are especially visible for very low-loss substrates. Further data processing can be applied to smooth the data of fit into, for example, one of the dielectric relaxation models. It is seen that above the TRL kit intended bandwidth, the extracted data starts to deteriorate. This is a combined result of fabrication and assembly tolerances together with repeatability as well as with the used SMA connector bandwidth. To assess the performance of the proposed method, the data for the reference substrate was compared with one obtained through the MDPL method and is provided in Fig. 4(a). Permeability is equal to unity while the measured permittivity aligns within $\Delta\varepsilon_r < 0.2$, $\Delta\tan\delta < 0.005$ for both methods. On the other hand, no data was found for the specialized material. The accuracy of the extracted ε_r and μ_r is linked to the uncertainties on the S-parameter measurements, repeatability of the TRL kit, dispersion of Z, the test line fabricated geometry (especially sample's thickness non-uniformity and length uncertainty) along with the accuracy of the effective to relative parameters model. Moreover, for low-loss materials,
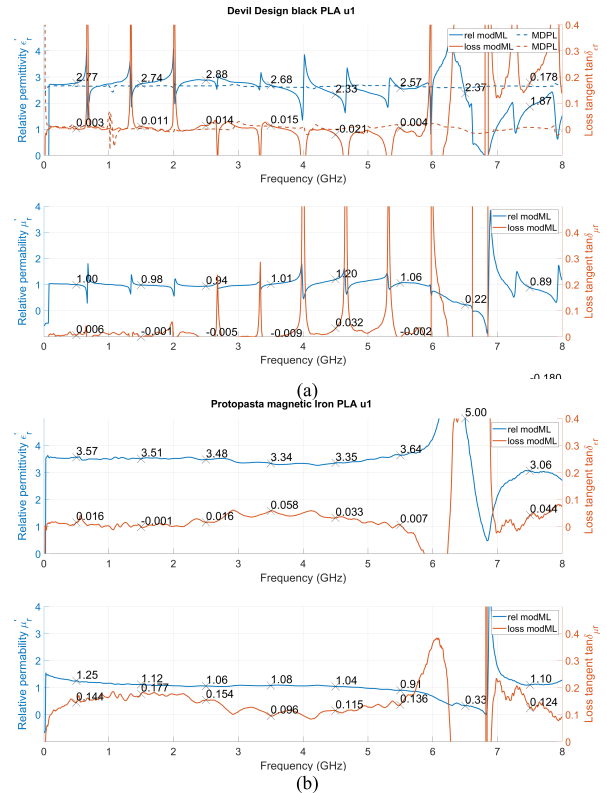

Fig. 4. Extracted complex relative permittivity and permeability for (a) black PLA dielectric substrate and (b) magnetic iron PLA magneto-dielectric substrate using the modML method (solid line). Plot (a) is overlaid with data for the MDPL (dashed line) as a reference.

the dielectric/magnetic, metallic, and radiation losses might be hard to separate. More detailed analysis can be found in, for example [15], [16].

It is seen from Fig. 4(b) that the Protopasta material indeed features both permittivity and permeability greater than unity. However, high magnetic losses are also visible that can be more than an order of magnitude higher than the dielectric ones in the sub-GHz range. High losses indicate that this filament might not be suited for practical applications of microwave circuits. Different infill print patterns and substrate thicknesses could be tested similar to study the affection of the above parameters of 3-D printed substrates. The developed technique enables fast assessment of substrate properties proving its usefulness. Moreover, the technique provides much detailed insights when compared to, for example [1] where post-fabrication electro-magnetic (EM) analysis was performed to determine substrate properties.

IV. CONCLUSION

A broadband microwave magneto-dielectric spectroscopy technique was introduced well suited for the characterization of 3-D printed magneto-dielectric substrates toward the realization of miniaturized and efficient RF electronics such as antennas. The all-printed test setup was introduced, and the data processing procedure was elaborated. The approach was experimentally validated on an example of two 3-D-printed substrates out of pure and doped PLA filaments. It was indicated that the setup can provide information on the influence of print parameters such as infill density and pattern or substrate thicknesses on the properties of the resulting substrate.

REFERENCES

[1] J. Sorocki, I. Piekarz, I. Slomian, S. Gruszczynski, and K. Wincza, "Realization of compact patch antennas on magneto-dielectric substrate using 3D printing technology with iron-enhanced PLA filament," in *Proc. Int. Conf. Electromagn. Adv. Appl. (ICEAA)*, Cartagena, Colombia, Sep. 2018, pp. 185–188.

[2] E. Andreou, T. Zervos, A. A. Alexandridis, and G. Fikioris, "Magnetodielectric materials in antenna design: Exploring the potentials for reconfigurability," *IEEE Antennas Propag. Mag.*, vol. 61, no. 1, pp. 29–40, Feb. 2019.

[3] K. Han *et al.*, "RF characterization of magnetodielectric material using cavity perturbation technique," *IEEE Trans. Compon., Packag., Manuf. Technol.*, vol. 5, no. 12, pp. 1850–1859, Dec. 2015.

[4] H.-Y. Gan *et al.*, "A CSRR-loaded planar sensor for simultaneously measuring permittivity and permeability," *IEEE Microw. Wireless Compon. Lett.*, vol. 30, no. 2, pp. 219–221, Feb. 2020.

[5] S. Arslanagić *et al.*, "A review of the scattering-parameter extraction method with clarification of ambiguity issues in relation to metamaterial homogenization," *IEEE Antennas Propag. Mag.*, vol. 55, no. 2, pp. 91–106, Apr. 2013.

[6] F. Costa *et al.*, "Electromagnetic characterisation of materials by using transmission/reflection (T/R) devices," *Electronics*, vol. 6, no. 4, p. 95, Nov. 2017.

[7] J. Hinojosa, "S-parameter broad-band measurements on-microstrip and fast extraction of the substrate intrinsic properties," *IEEE Microw. Wireless Compon. Lett.*, vol. 11, no. 7, pp. 305–307, Jul. 2001.

[8] *Anritsu Universal Test Fixtures 3680 Series*. Accessed: Feb. 15, 2021. [Online]. Available: https://www.anritsu.com/en-us/components-accessories/products/3680-series

[9] G. F. Engen and C. A. Hoer, "Thru-reflect-line: An improved technique for calibrating the dual six-port automatic network analyzer," *IEEE Trans. Microw. Theory Techn.*, vol. I-27, no. 12, pp. 987–993, Dec. 1979.

[10] E. Hammerstad and O. Jensen, "Accurate models for microstrip computer-aided design," in *IEEE MTT-S Int. Microw. Symp. Dig.*, May 1980, pp. 407–409.

[11] M. Kirschning and R. H. Jansen, "Accurate model for effective dielectric constant of microstrip with validity up to millimetre-wave frequencies," *Electron. Lett.*, vol. 18, pp. 272–273, Jun. 1982.

[12] *Devil Design PLA Filament*. Accessed: Feb. 15, 2021. [Online]. Available: https://devildesign.com/oferta/

[13] J. A. Reynoso-Hernandez, "Unified method for determining the complex propagation constant of reflecting and nonreflecting transmission lines," *IEEE Microw. Wireless Compon. Lett.*, vol. 13, no. 8, pp. 351–353, Aug. 2003.

[14] *Protopasta Iron-filled Metal Composite PLA Filament*. Accessed: Feb. 15, 2021. [Online]. Available: https://www.proto-pasta.com/products/magnetic-iron-pla

[15] N. K. Das, S. M. Voda, and D. M. Pozar, "Two methods for the measurement of substrate dielectric constant," *IEEE Trans. Microw. Theory Techn.*, vol. I-35, no. 7, pp. 636–642, Jul. 1987.

[16] A.-H. Boughriet, C. Legrand, and A. Chapoton, "Noniterative stable transmission/reflection method for low-loss material complex permittivity determination," *IEEE Trans. Microw. Theory Techn.*, vol. 45, no. 1, pp. 52–57, Jan. 1997.